


Article

Impact of Grinding of Printed Circuit Boards on the Efficiency of Metal Recovery by Means of Electrostatic Separation

Tomasz Suponik ^{1,*}, Dawid M. Franke ¹, Paweł M. Nuckowski ², Piotr Matusiak ³, Daniel Kowol ³
and Barbara Tora ⁴

- ¹ Institute of Mining, Faculty of Mining, Safety Engineering and Industrial Automation, Silesian University of Technology, 2 Akademicka Street, 44-100 Gliwice, Poland; dawid.franke@polsl.pl
- ² Materials Research Laboratory, Faculty of Mechanical Engineering, Silesian University of Technology, 18A Konarskiego Street, 44-100 Gliwice, Poland; pawel.nuckowski@polsl.pl
- ³ KOMAG Institute of Mining Technology, 37 Pszczynska, 44-101 Gliwice, Poland; pmatusiak@komag.eu (P.M.); dkowol@komag.eu (D.K.)
- ⁴ Faculty of Mining and Geoengineering, AGH University of Science and Technology, 30 Mickiewicza, 30-059 Kraków, Poland; tora@agh.edu.pl
- * Correspondence: tomasz.suponik@polsl.pl

Abstract: This paper analyses the impact of the method of grinding printed circuit boards (PCBs) in a knife mill on the efficiency and purity of products obtained during electrostatic separation. The separated metals and plastics and ceramics can be used as secondary raw materials. This is in line with the principle of circular economy. Three different screen perforations were used in the mill to obtain different sizes of ground grains. Moreover, the effect of cooling the feed to cryogenic temperature on the final products of separation was investigated. The level of contamination of the concentrate, intermediate, and waste obtained as a result of the application of fixed, determined electrostatic separation parameters was assessed using ICP-AES, SEM-EDS, XRD, and microscopic analysis as well as specific density. The yields of grain classes obtained from grinding in a knife mill were tested through sieve analysis and by using a particle size analyser. The test results indicate that using a knife mill with a 1 mm screen perforation along with cooling the feed to cryogenic temperature significantly improves the efficiency of the process. The grinding products were characterised by the highest release level of the useful substance—metals in the free state. The purity of the concentrate and waste obtained from electrostatic separation was satisfactory, and the content of the intermediate, in which conglomerates of solid metal–plastic connections were present, was very low. The yield of concentrate and waste amounted to 26.2% and 71.0%, respectively. Their purity, reflected in the content of the identified metals (valuable metals), was at the level of 93.3% and 0.5%, respectively. In order to achieve effective recovery of metals from PCBs by means of electrostatic separation, one should strive to obtain a feed composed of grains <1000 µm and, optimally, <800 µm.

Keywords: metals recovery; printed circuit board; cryogenic grinding; electrostatic separation; atomic emission spectroscopy; scanning electron microscopy (SEM); X-ray diffraction (XRD)



Citation: Suponik, T.; Franke, D.M.; Nuckowski, P.M.; Matusiak, P.; Kowol, D.; Tora, B. Impact of Grinding of Printed Circuit Boards on the Efficiency of Metal Recovery by Means of Electrostatic Separation. *Minerals* **2021**, *11*, 281. <https://doi.org/10.3390/min11030281>

Academic Editors: Zenixole Tshentu and Durga Parajuli

Received: 20 January 2021

Accepted: 2 March 2021

Published: 9 March 2021

Publisher's Note: MDPI stays neutral with regard to jurisdictional claims in published maps and institutional affiliations.



Copyright: © 2021 by the authors. Licensee MDPI, Basel, Switzerland. This article is an open access article distributed under the terms and conditions of the Creative Commons Attribution (CC BY) license (<https://creativecommons.org/licenses/by/4.0/>).

1. Introduction

In line with the circular economy principle, and for economic and environmental reasons, the recovery of metals from printed circuit boards (PCBs) is not only required—it is obligatory. The production process created for this purpose should be characterised by high efficiency, low costs, and a low impact on the natural environment. The method for preparing PCBs for separation processes is crucial in terms of purity and efficiency of the products obtained. The correct method for PCB grinding can facilitate the full release of useful components (i.e., metals in the free state) to produce pure concentrate in the separation processes and minimise the effect of penetration of metals into waste.

According to Vermesan et al. [1], PCB recycling directions should include disassembly (i.e., removal of hazardous products, such as batteries and capacitors), treatment (i.e.,

reduction of PCB dimensions), and finally, processing of the obtained products. This approach can provide economic and environmental benefits in the recovery of metals, but also of plastics and ceramics from PCBs.

The rapid advancement of computer technologies has contributed to a change in consumption patterns, which has resulted in a mass replacement of devices with new ones with much higher efficiencies [2]. In 2019, 53.6 million tonnes of electronic waste was generated. It is 9.2 million tonnes more compared with that in 2014 [3]. As a result, even greater amounts of waste electrical and electronic equipment (WEEE) are generated. They contain toxic heavy metals and halogenated flame retardants [4], which may penetrate into the aquatic environment. One of the basic building blocks of WEEE are PCBs [2]. Their content of metals is significantly higher than in natural metal ores [5–8]. PCBs are composed of about 30% metals in the free state and about 70% components, such as glass fibre, epoxy resin, and polyester. For the sake of simplicity, these components of PCBs are hereinafter referred to as plastic and ceramic materials [9,10]. Depending on the material used to build the laminate (dielectric materials), there are many types of PCBs, such as FR-2 to 6, G-10, G-11, and CEM-1 to 8 [10,11]. The most common type is FR-4, whose laminate mainly consists of epoxy resin reinforced with glass fibres and SiO₂ (approximately 40%), CaO (approximately 20%), and smaller amounts of Al₂O₃, MgO, and BaO [12]. This type of boards allows for the use of high operating temperatures (130 °C and above). To improve this property of PCBs, flame retardants are used, which include bromine and antimony compounds [11,13]. PCBs, depending on the manufacturer, production date, and destination, exhibit different metal contents. The estimated contents of noble (Au, Ag, and Pd) and seminoble (Cu) metals in PCBs are 0.05%, 0.03%, 0.01%, and 16%, respectively. Moreover, other metals occur in small concentrations in PCBs: 3% Fe, 3% Sn, 2% Pb, 1% Zn, and trace amounts of Al, Ni, Cr, Na, Cd, Mo, Ti, and Co [10,14,15]. Due to their properties, noble metals have found their application in the production of PCBs, mainly as contact metals [16]. Gold is used in bonding wires, contacts, and integrated circuits. Silver is used as contacts, switches, and solders, while palladium and platinum are used for multilayer capacitors and connectors as well as hard disks, thermocouples, and fuel cells, respectively [17]. As a seminoble (but the most abundant) metal, copper is used in the production of cables, wires, connectors, and other components [17]. The amount of precious metals, such as gold, silver, and palladium, contained in e-waste is increasing rapidly, with used mobile phones having the largest share [18]. According to the work of Hagelüken [19], about 350 g/t Au, 1380 g/t Ag, and 210 g/t Pd are present in PCBs and other components of mobile phones.

E-waste raw materials were estimated to be worth USD 57 billion in 2019. This concerns about 17% of e-waste documented in that year. The value of the processed waste can be estimated to be about USD 10 billion. However, the processing of about 83% of e-waste generated in 2019 was not documented, which contributed to environmental interference and the impact on employees' health [3,20]. Therefore, proper recycling of WEEE is necessary, not only for the protection of the environment and natural resources, but also for economic reasons, creation of new jobs, and reduction of the impact of landfills on the landscape [21,22].

The methods for recovering metals from PCBs can be divided into physical and chemical methods [23], including the use of microorganisms (bioleaching) [24]. Some of the chemical ones, especially pyro- and hydro-metallurgical methods, have a significant impact on the natural environment, including water and air pollution and waste generation [25–27]. Compared with other chemical methods, bioleaching has a negligible impact on the environment; however, these are long-term methods [28]. Therefore, the possibility of using known, cheap, and environmentally friendly solutions is being analysed. These certainly include the methods of grinding and electrostatic separation.

The efficiency of metal recovery using these methods depends on the degree of metal release. Therefore, in order to ensure high efficiency of electrostatic separation, PCBs should be ground to release the useful components (i.e., metals) from plastic and ceramic

materials. This process is characterised by high energy consumption [9,29]. PCBs are characterised by a complicated structure, as they are composed of many conductive layers (mainly copper) placed on nonconductive substrates [24,30]. Each component may consist of various elements mechanically connected with each other [31,32]. Additionally, the materials used in PCBs are characterised by varied mechanical properties. Most boards have a glass fibre substrate that breaks easily when shear forces are applied. Selective grounding of PCBs can be performed in knife or hammer mills [22,33]. In order to adjust the process, multistage grinding or grinding with liquid nitrogen can be used [22,33–35].

The recovery of metals from PCBs with the use of electrostatic separation has already found application in some places of the globe [8,36–38]. It consists of grain separation due to the differences in the ability to accumulate surface charges and electric current conductivity properties [29,39,40]. The literature contains two main solutions for the construction of electrostatic separators: drum and free-fall electrostatic separators [41,42]. In the case of drum separators, the separation efficiency depends on the voltage, the rotational speed of the drum, the electrode position, and the feed efficiency (separator load) [43,44]. The selection of separation parameters depends mainly on the design of the device and grain size. With the inappropriate selection of parameters, electrostatic separation will not be effective and may even damage the electrode through spark discharge [40]. Large grains are often combinations of metals with plastic and ceramic materials, and thus the efficiency of metal recovery from PCBs may be low [36,45]. Depending on the conditions of the separation process, the type of feed fed to the separator, the following product ranges can be obtained: 9%–27% conductive grains (metals), 2%–6% mixed grains, and 67%–85% nonconductive grains [38,43].

The aim of the study was to assess the impact of the PCB grinding method in a knife mill on the purity of products obtained during electrostatic separation. The level of contamination of the concentrate, intermediate, and waste obtained as a result of the application of fixed, determined electrostatic separation parameters was assessed using inductively coupled plasma atomic emission spectroscopy (ICP-AES), specific density analysis using a pycnometer and ethyl alcohol (PN-EN 1097-7 No. 2001), scanning electron microscope (SEM) with energy dispersive X-ray spectroscopy (EDS), microscopic analysis using stereo microscope, and X-ray powder diffraction (XRD).

2. Materials and Methods

2.1. Grinding Materials and Methods

Motherboards manufactured by Gigabyte, Intel, Nvidia, MSI, and Asus in 2007–2009 were used in the tests. These are the most common FR-4 boards, the laminate of which is made of fibre glass with epoxy resin [31,46]. Before commencing the grinding, the boards were manually disassembled with the use of workshop tools (screwdrivers and pliers) [47], and components of a different physical and chemical nature, which could have disturbed the process of grinding and electrostatic separation, were easily removed. These components included resistors (Ni, Cr, Cd, Al, Pb, and Ta), transistors (Pb and Cu), batteries, chips (Pb, Ni, Sn, Ga, Al, and Ag), capacitors (Sn, Cu, and Zn), electromagnetic interference filters (Fe, Cu, and Zn), connectors (Pb, Ni, and Sn), screws, and switches [48].

A LMN-100 knife mill from Testchem (Radlin, Poland) [49] was used in the grinding processes. In mills of this type, the grinding takes place by cutting the material by knives mounted on the device body and a rotator. These mills are equipped with a screen to determine the size of the ground material. The feed to the mill were PCBs cut into 3×3 cm pieces. The following different process conditions (options) were used to produce the grinding product in different grain classes:

- option 1—1 mm screen perforation, mill load (capacity of feeding the material to the mill): 5 g/min;
- option 2—1 mm screen perforation, cooling the feed with liquid nitrogen, mill load: 20 g/min;
- option 3—2 mm screen perforation, mill load: 10 g/min;

- option 4—3 mm screen perforation, mill load: 10 g/min.

The other process parameters remained unchanged and were as follows:

- rotator speed: 2815 min^{−1};
- gap between the knives in the mill: 0.5 mm.

During the PCB grinding, the mill was not allowed to overload, which could contribute to high temperatures in the grinding working chamber, causing the formation of conglomerates—solid metal–plastic–ceramic compounds. Therefore, different mill loads were used in different options. Despite this, it was noticed that the temperature in the working chamber of the mill was increasing. In option 2, liquid nitrogen was used to reduce the temperature of the ground PCBs to the level of cryogenic temperatures (below −150 °C). The cooling process consisted in placing the feed into a container filled with liquid nitrogen. The feed was cooled until liquid nitrogen ceased to boil.

2.2. Electrostatic Separation

In order to recover metals from ground PCBs, electrostatic separation was used consisting in grain separation due to differences in the ability to accumulate surface charges and the properties of electric current conductivity [29,39,40]. The tests were carried out in a drum electrostatic separator from Boxmag-rapid Ltc. (Aston, Birmingham, UK), which allows for a three-product separation into waste, intermediate, and concentrate. The design of the device allows for the optimisation of the separation conditions by means of changing the rotational speed of the shaft (i.e., the material feeding efficiency, the voltage flowing through the electrode, and its distance from the shaft). The diagram and structure of the device is shown in Figure 1.

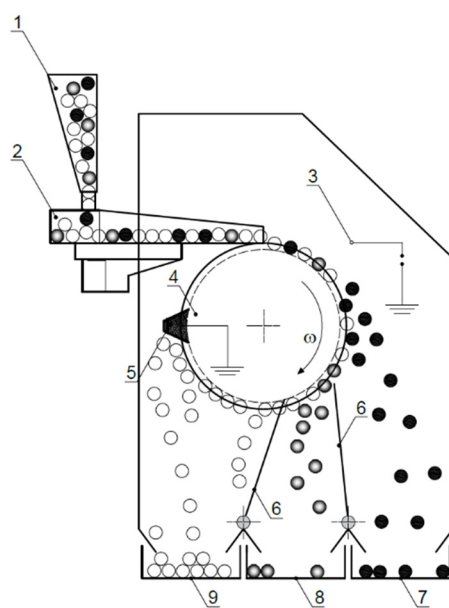


Figure 1. Diagram of the electrostatic separator: 1—feed container, 2—vibrating feeder, 3—electrode, 4—drum, 5—brush, 6—partition, 7—conductor container (concentrate), 8—container for complex grains folded with metals and nonmetals, and 9—nonconductor container (waste).

In the case of perfect separation, grains with good electrically conductive properties (e.g., metals in the free state) will be the first to detach from the drum to form a concentrate, while nonconductive grains (plastics and ceramics) will detach last or will be pulled off with a brush, creating waste. Grains that show moderate conductive properties or poor capacity to accumulate surface charges (e.g., solid metal–plastic–ceramic compounds) will detach between the concentrate and the waste and form the intermediate. On the basis of preliminary tests and previous studies by Suponik and Franke [50,51], it was decided that

electrostatic separation, aimed at selecting the optimal option of PCB grinding, would be performed for the following technical parameters: shaft rotation speed of 100 rpm, voltage of 17 kV, distance between electrode and drum of 0.03 m.

2.3. Product Analysis

After PCB grinding, particle size analysis of the obtained material was carried out using the following:

- Fritsch screens with mesh sizes of 2 mm, 1.4 mm, 1 mm, 710 μm , 500 μm , 355 μm , 250 μm , 180 μm , 125 μm , and 90 μm .
- ANALYSETTE 22 MicroTec Plus Laser Particle Sizer (Fritsch, Idar-Oberstein, Germany)—the measurement was not carried out on material obtained from grinding in a mill with a screen with 2 and 3 mm perforation due to limitations in the measurement of grain size.

Two methods of analysis were used in the study, as the grains had different sizes, shapes, and wettability. In the particle size analyser, the tiniest hardly wettable particles, occurring in low amounts, were removed prior to the analysis.

The electrostatic separation products obtained for the analysed options of PCB grinding were analysed via the following:

- ICP-AES—using the JY2000 Optical Emission Spectrometer (by Jobin Yvon) in order to assess the content of elements in products. The source of the induction was a plasma torch coupled with a 40.68 MHz frequency generator; the products were previously dissolved.
- Specific density analysis—using Gay-Lussac pycnometers on the basis of PN-EN 1097-7:2001 with the use of ethyl alcohol with a density of 0.7893 g/cm³.
- Microscope analysis with Zeiss SteREO Discovery Modular Stereo Microscope (Carl Zeiss AG, Jena, Germany).

For the best selected option of PCB grinding, the obtained concentrate and intermediate were subsequently analysed using the following:

- High-resolution Zeiss SUPRA 35 scanning electron microscope (Carl Zeiss AG, Germany), equipped with EDAX energy dispersive X-ray spectroscopy (EDS) chemical analysis system (EDAX, Mahwah, NJ, USA).
- Qualitative phase analysis was performed with the use of a Panalytical X'Pert Pro MPD diffractometer (Panalytical, Almelo, The Netherlands), utilising filtered radiation of a cobalt anode lamp ($\lambda_{K\alpha} = 0.179 \text{ nm}$). The diffraction lines were recorded in the Bragg–Brentano geometry, using the step-scanning method by means of a PIXcell 3D detector on the diffracted beam axis, in the angle range of 20°–100° [2 θ] (step, 0.05°; count time per step, 200 s). The obtained diffractograms were analysed with the use of Panalytical HighScore Plus (v. 3.0e) software with the PAN-ICSD database.

Due to the presence of large amounts of plastics in the feed and waste from electrostatic separation and the possibility of damaging the equipment, SEM-EDS and XRD analyses were not performed for these products.

3. Results

3.1. Grinding

The results of the grain analysis of the PCBs ground in a knife mill for various process options are presented in Table 1. Due to the fibrous/needle shape of the ground grains of epoxy resin and glass fibre (Figure 2) and various shapes of the fragmented metal particles (Figures 3 and 4), it was difficult to unambiguously determine and assess the grain size.

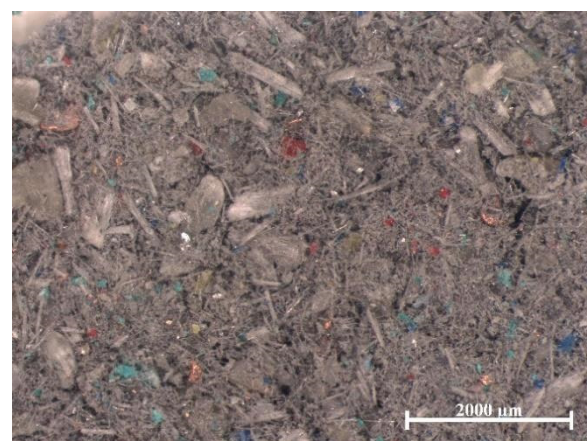
Table 1. Yield of grinding product grain classes.

Grain Class, mm	Yield of Product, %					
	Option 1 ^a	Option 1 ^b	Option 2 ^a	Option 2 ^b	Option 3 ^a	Option 4 ^a
>2.0	0.0	0.0	0.0	0.0	0.0	0.2
2.0–1.4	0.0	0.0	0.0	0.0	0.4	13.7
1.4–1.0	0.3	0.0	0.4	0.0	11.1	24.6
1.0–0.71	5.7	5.2	3.6	1.6	25.6	16.8
0.71–0.50	14.1	14.8	13.0	10.4	15.6	10.7
0.50–0.36	19.3	22.0	19.5	22.1	11.6	8.4
0.36–0.25	17.0	10.4	17.0	14.2	8.6	6.3
0.25–0.18	9.6	5.6	10.6	6.5	5.0	4.1
0.18–0.13	8.5	4.9	10.8	5.3	4.5	4.5
0.13–0.09	9.1	3.8	8.5	4.3	3.6	4.2
<0.09	16.3	33.3	16.6	35.6	13.9	6.5

^a analysis carried out with Fritsch screens, ^b analysis carried out with the particle size analyser.



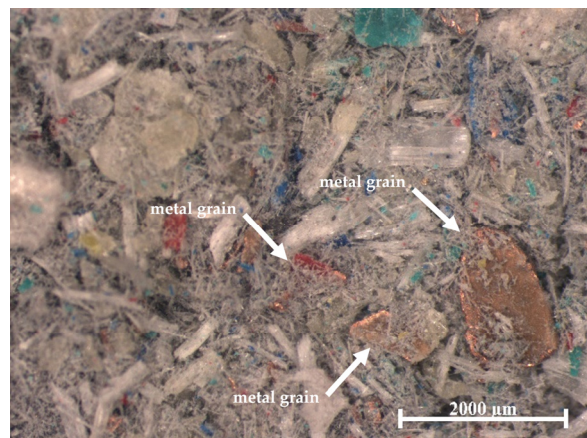
(a)



(b)

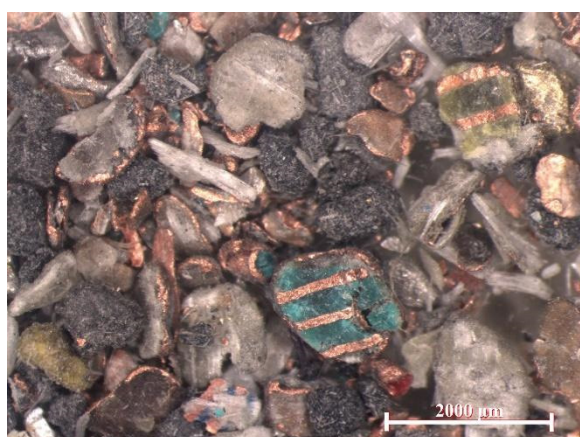


(c)

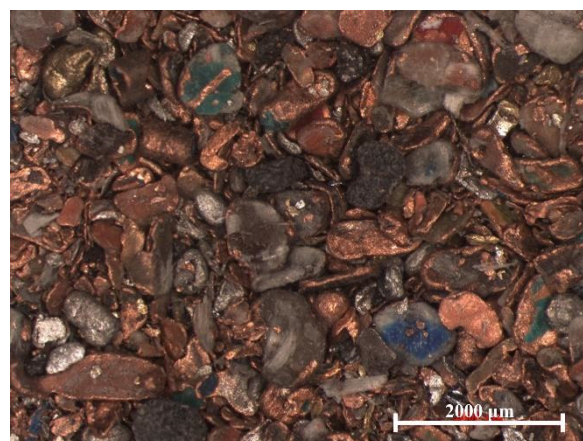


(d)

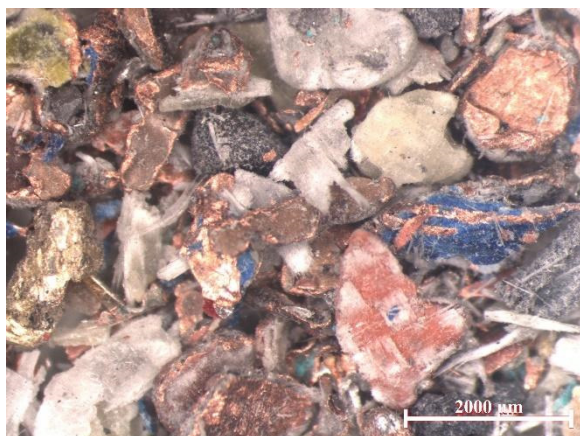
Figure 2. Waste from electrostatic separation (stereo microscope): (a) option 1, (b) option 2, (c) option 3, and (d) option 4.



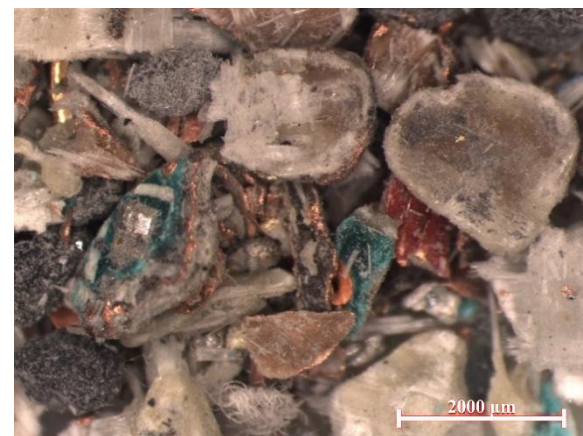
(a)



(b)

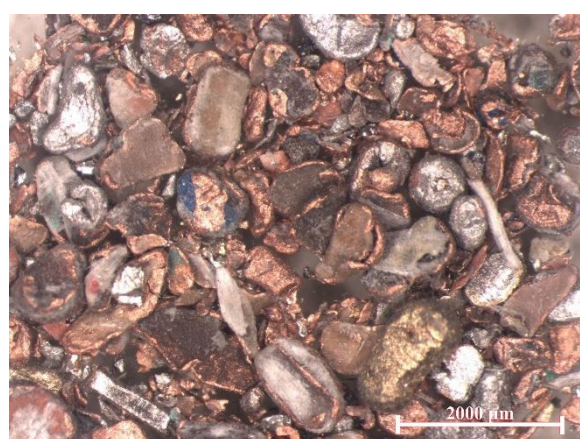


(c)

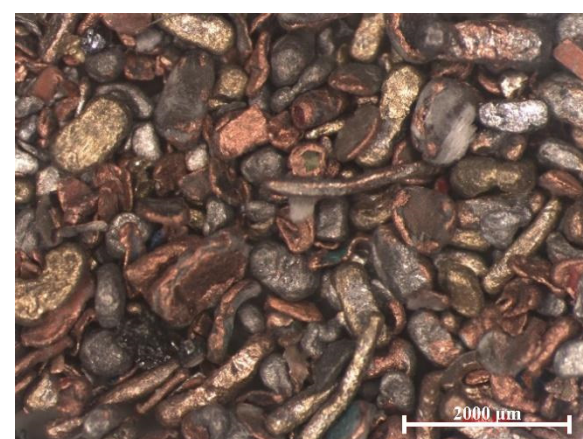


(d)

Figure 3. Intermediate from electrostatic separation (stereo microscope): (a) option 1, (b) option 2, (c) option 3, and (d) option 4.



(a)



(b)

Figure 4. *Cont.*

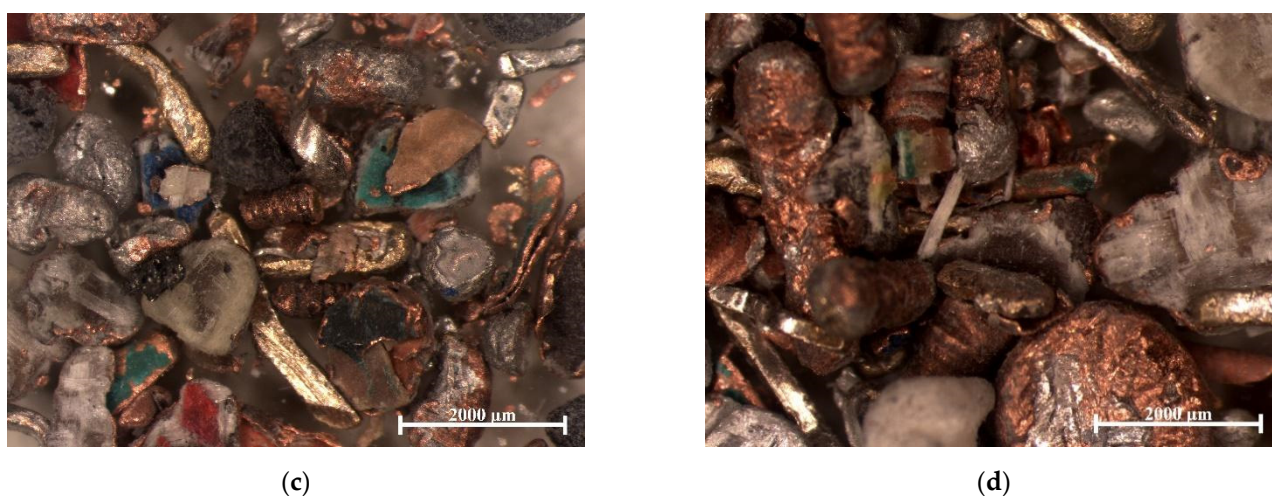


Figure 4. Concentrate from electrostatic separation (stereo microscope): (a) option 1, (b) option 2, (c) option 3, and (d) option 4.

As could be expected, however, with the increase of the screen perforation in the knife mill (options 3 and 4), the material obtained after grinding was characterised by larger grain sizes. The largest content in options 3 and 4 was represented by 1.4–0.355 mm and 2.0–0.5 mm grain classes, respectively (Table 1). For options 1 and 2 (i.e., with the use of a screen with a 1 mm perforation), respectively, without and with cooling the feed to cryogenic temperatures, the shredded material was obtained mainly in classes from 1.0 to 0.25 mm and <0.09 mm, while for option 2, the grains were generally slightly smaller (Table 1). For example, material with a size <0.5 mm was represented at 88% for this option and at 80% for option 1. The differences in the results between the sieve analysis and the particle size analyser are due to the different shapes of the grains. For metals, the grains were mainly globular, patch, and needle shaped, and for plastic and ceramic materials, fibrous and patch shaped.

3.2. Analysis of the Electrostatic Separation Efficiency

Based on the density of the products obtained from electrostatic separation (Table 2), it can be concluded that its efficiency, manifested by the purity of the concentrate (the presence of metals with a minimum amount of plastic and ceramic materials) and waste (the presence of plastic and ceramic materials with a minimum amount of metals), increases with the degree of PCB grinding. The higher the density of the separation product, the higher the metal content and the lower the plastic and ceramic content. The highest and lowest densities of the concentrate and the lowest and highest densities of waste were obtained for options 2 and 4, respectively. This is correlated with the grain size, which in turn is related to the release of useful components (i.e., metals). A high purity of the concentrate and waste was also achieved for option 1. However, at low temperatures (option 2 of the grinding process), due to the use of liquid nitrogen to cool the feed, there was no significant increase in temperature in the mill's working chamber, and no plasticisation of the shredded material, and no (or less) solid metal–plastic–ceramic compounds.

Table 2. Yield and density of electrostatic separation products.

Grinding Option	Yield of Product, %			Density, g/cc		
	Waste	Intermediate	Concentrate	Waste	Intermediate	Concentrate
Option 1	71.5	2.8	25.8	2.61	5.98	8.78
Option 2	71.0	2.8	26.2	2.29	5.33	8.87
Option 3	66.7	6.1	27.2	2.92	3.76	7.32
Option 4	50.4	6.3	43.2	3.35	3.5	5.51

However, the yield of concentrates and intermediates in options 1 and 2 is the lowest. In both cases, as previously noted, the presence of plastic and ceramic materials was minimised. The most concentrate and the least waste were obtained for option 4. However, taking into account the densities of plastics, ceramics, and metals, it is concluded that the separation products for option 4 are highly contaminated. This is due to the low degree of grinding, which did not allow the sufficient release of useful substances (metals in the free state) from the PCB composite.

Figures 2–4 present pictures of the waste, intermediate, and concentrate (made with a stereo microscope), respectively, from the electrostatic separation process obtained for different grinding options. They confirm that the sizes of all grains decreased along with the reduction of perforation in the knife mill screens. Using additional cooling of the feed in option 2, the smallest grain sizes were obtained, which is particularly noticeable for the intermediate (Figure 3b).

In the waste for all grinding options (Figure 2), there were small amounts of metal grains or metal–plastic–ceramic conglomerates, while in the intermediates (Figure 3), there were many grains that clearly indicated these compounds. The waste (Figure 2) consisted mainly of fibrous and needle-shaped grains. Compared with other separation products, the greatest diversity of grains was observed in terms of their size, from less than 50 μm (fibre/needle thickness) to over 2000 μm . However, in the waste for options 1 and 2, grains larger than 1000 μm were relatively the scarcest. The penetration of grains larger than the screen used in the mill resulted from the elongated shape of the grains. The intermediates (Figure 3) consisted mainly of patch grains and globular grains. The grains presented in Figure 3c,d have a layer structure characteristic of PCBs. This shows that the level of grinding is insufficient. For option 2, the grain size was the least diversified (Figure 2b). There were mainly thin patch grains with a diameter of 150 to 1000 μm . The yield of intermediates for options 1 and 2 was, however, very small, amounting to 2.8%. This shows that only a small fraction of the metals was not released sufficiently in the grinding process. In the intermediate of option 2, the least compounds of this type are observed, which may indicate the highest degree of release of the useful substance from the composite among the options. This part can be recycled for further grinding or processed using other metal recovery methods, such as bioleaching [28,52].

For the concentrates obtained in the third and fourth grinding options (Figure 4c,d), numerous metal–plastic–ceramic compounds are visible, which is not the case for option 1 (Figure 4a), and especially option 2 (Figure 4b). In the group of all concentrates (Figure 4), the greatest differentiation in terms of grain shape can be observed. There were polyhedral, globular, patch, and irregular grains here. The concentrate for option 2 (Figure 4b), as compared with the others, was characterised by the smallest differentiation in terms of grain size and shape (the grains were more rounded). This shows that the strength properties of PCBs have changed at cryogenic temperatures due to the application of liquid nitrogen. Option 2 was dominated by grains of globular shape (most abundant in the range of 250–500 μm) and patch shape (patch thickness, >30 μm ; width, ~500 μm). In the case of polyhedral grains, the transverse dimensions ranged from 200 to 350 μm . Irregular grains were probably created as a result of crushing the patch grains.

In order to improve the efficiency of electrostatic separation, the process can be optimised by adjusting the voltage applied to the electrode, the distance between the electrode and the device's shaft, and the shaft rotation speed. Failure to adjust the last of the mentioned parameters could cause very fine metal particles to penetrate into the intermediate and waste. These particles were affected by a very small centrifugal force due to the movement of the separator shaft.

The grains of metals, probably copper, with dimensions of 450, 800, and 1200 μm , visible in Figure 2a,d, characterised by a patch shape, could have penetrated into the waste and the intermediate due to the presence of plastic and ceramic materials in the grain or as a result of being covered by grains made of plastic and ceramic materials (aggregation effect) [36]. The results of the tests of the chemical compositions of the feed

and electrostatic separation products for all analysed grinding options are presented in Table 3 (the measurements were made using ICP-AES). In the feed, the main identified elements were Cu (17.70%), Si (12.02%), Ca (6.56%), Sn (2.92%), Al (1.95%), Br (1.64%), and less than 1% of Zn, Mg, Pb, Fe, Ba, Ti, Sb, Ni, Cr, Mn, and Ag (0.0301%), and Au (0.0029%). The remaining unidentified part of the feed probably consists of the components of epoxy resins, which mainly include polyphenols, less often polyglycols, and epichlorohydrin or oligomers [53–55].

Concentrates obtained from electrostatic separation, first, second, third, and fourth grinding options, contained 86.6%, 93.3%, 76.0%, and 54.4% of valuable metals, respectively, among which for the most effective option 2, 68.5% Cu, 0.1074% Ag, 0.0142% Au, and 2.7%, 2.0%, 9.6%, and 9.8% residues constituting nonvaluable elements were identified. The second group of elements includes Sb, Ca, Br, Ba, Mg, Mn—components of epoxy resins used to improve the properties of PCBs, especially as flame retardants [12]—and Si, a component of glass fabrics [10].

In the concentrate for option 2, the share of precious metals was clearly visible, which was 0.1074% for silver and 0.0092% for gold. The most abundant metal in the concentrate was copper (68.5%), followed by tin (11.5%) and aluminium (6.8%). Higher amounts of metals as compared with the other options also applied to metals such as zinc, magnesium, lead, barium, calcium, iron, nickel, titanium, and chromium.

As can be seen above, the concentrate obtained from option 2 contained much larger amounts of valuable metals than those from options 3 and 4 and slightly larger amounts than that from option 1. This demonstrates that the efficiency of the electrostatic separation process is influenced by the method of preparing the feed for the separator—first, the perforation in the knife mill screen, and then the cooling of the feed to the knife mill to cryogenic temperatures.

The yield of intermediates from the electrostatic separation process ranged, for the tested options of PCB grinding, from 2.8% for options 1 and 2 to 6.3% for option 4 (Table 2). This is a small amount, especially for the first two grinding options. The ICP tests identified 22% (option 2) to 27% (option 3) of elements. The remaining part are probably, as for the remaining separation products, organic substances in the form of the previously mentioned polyphenols or polyglycols. Of the identified elements, 45%–60% were valuable elements. For the most effective grinding option, they were Cu (6.68%), Fe (1.50%), Al (1.34%), and Sn (1.18%). Among the nonvaluable elements, Si (3.19%), Ca (2.41%), Mg (1.51%), and Br (1.12%) should be mentioned.

There were small amounts of metals in the waste from electrostatic separation, especially in options 1 (1.99%) and 2 (0.54%). In this end product, apart from unidentified organic substances, Si (approximately 14%) and Ca (approximately 8%) as well as Mg and Br (approximately 2%) were identified. The waste yield in option 2 was as high as 71%. Taking into account the fact that there were almost no metals in the free state, it can be used for the production of various components/prefabricates [12].

Table 3. Elemental content in the feed and electrostatic separation products for all grinding options.

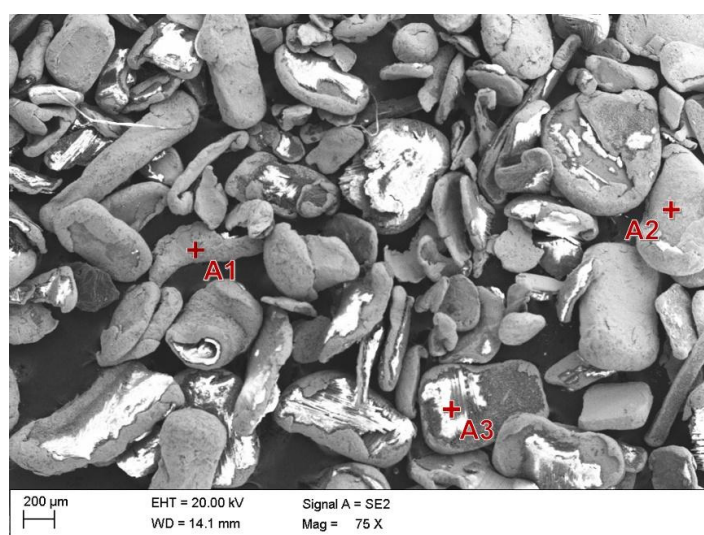
Element		Content of the Element, %, in												
		Feed	Concentrate				Intermediate				Waste			
			Option 1	Option 2	Option 3	Option 4	Option 1	Option 2	Option 3	Option 4	Option 1	Option 2	Option 3	Option 4
Valuable elements	Cu	17.70 ± 1.77	64.17 ± 6.42	68.50 ± 6.85	54.29 ± 5.43	38.45 ± 3.85	5.14 ± 0.51	6.68 ± 0.67	6.42 ± 0.64	7.47 ± 0.75	1.24 ± 0.12	0.17 ± 0.02	3.20 ± 0.32	3.89 ± 0.39
	Al	1.95 ± 0.20	5.28 ± 0.53	6.82 ± 0.68	4.58 ± 0.46	4.08 ± 0.41	1.18 ± 0.12	1.34 ± 0.13	0.84 ± 0.08	0.54 ± 0.05	0.2 ± 0.02	0.07 ± 0.01	0.48 ± 0.05	0.29 ± 0.03
	Pb	0.39 ± 0.04	2.04 ± 0.20	1.5 ± 0.15	2.54 ± 0.25	1.74 ± 0.17	1.28 ± 0.13	0.74 ± 0.07	0.47 ± 0.04	0.08 ± 0.01	BDL *	0.001 ± 0.0001	BDL *	0.02 ± 0.002
	Zn	0.69 ± 0.07	1.22 ± 0.12	2.5 ± 0.25	1.87 ± 0.19	0.87 ± 0.09	0.74 ± 0.07	0.94 ± 0.09	0.40 ± 0.04	0.94 ± 0.09	0.14 ± 0.01	BDL *	0.08 ± 0.01	BDL *
	Ni	0.19 ± 0.02	1.28 ± 0.13	0.75 ± 0.08	0.49 ± 0.05	0.34 ± 0.03	0.75 ± 0.07	0.31 ± 0.03	0.41 ± 0.04	0.21 ± 0.02	BDL *	BDL *	0.18 ± 0.02	BDL *
	Fe	0.38 ± 0.04	2.42 ± 0.24	0.95 ± 0.10	1.87 ± 0.19	1.11 ± 0.11	0.61 ± 0.06	1.50 ± 0.15	1.64 ± 0.16	0.84 ± 0.08	0.04 ± 0.004	0.09 ± 0.01	0.15 ± 0.02	0.40 ± 0.04
	Sn	2.92 ± 0.29	9.54 ± 0.95	11.5 ± 1.15	9.78 ± 0.98	7.21 ± 0.72	2.57 ± 0.26	1.18 ± 0.12	1.88 ± 0.19	0.58 ± 0.06	0.15 ± 0.02	0.02 ± 0.002	1.14 ± 0.11	1.19 ± 0.12
	Cr	0.06 ± 0.06	0.18 ± 0.02	0.15 ± 0.02	0.09 ± 0.01	0.04 ± 0.004	0.02 ± 0.002	0.04 ± 0.004	0.47 ± 0.05	0.27 ± 0.03	0.001 ± 0.0001	0.001 ± 0.0001	BDL *	0.04 ± 0.004
	Ti	0.26 ± 0.03	0.39 ± 0.04	0.51 ± 0.05	0.51 ± 0.05	0.51 ± 0.05	BDL *	0.39 ± 0.04	0.40 ± 0.04	0.22 ± 0.02	0.21 ± 0.02	0.18 ± 0.02	0.28 ± 0.03	BDL *
	Ag	0.030 ± 0.003	0.0647 ± 0.0067	0.1074 ± 0.0011	0.0221 ± 0.0022	0.0054 ± 0.0005	BDL *	BDL *	0.0007 ± 0.0001	BDL *	BDL *	BDL *	BDL *	0.0002 ± 0.00002
	Au	0.0029 ± 0.0003	0.0010 ± 0.0001	0.0092 ± 0.0009	0.0005 ± 0.0001	0.0007 ± 0.0001	BDL *	BDL *	BDL *	BDL *	BDL *	BDL *	BDL *	BDL *
Sum		24.57	86.58	93.30	76.04	54.36	12.29	13.12	12.93	11.15	1.99	0.54	5.51	5.83

Table 3. Cont.

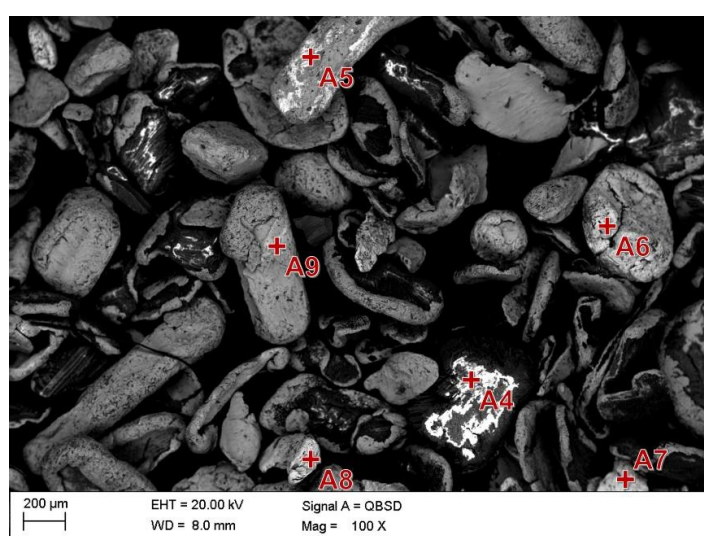
Element		Content of the Element, %, in												
		Feed	Concentrate				Intermediate				Waste			
			Option 1	Option 2	Option 3	Option 4	Option 1	Option 2	Option 3	Option 4	Option 1	Option 2	Option 3	Option 4
Nonvaluable elements	Sb	0.22 ± 0.02	0.27 ± 0.03	0.61 ± 0.06	0.19 ± 0.02	0.08 ± 0.01	BDL *	0.18 ± 0.02	0.18 ± 0.02	0.12 ± 0.01	0.21 ± 0.02	0.01 ± 0.001	0.27 ± 0.03	0.33 ± 0.03
	Ca	6.56 ± 0.66	0.98 ± 0.10	0.92 ± 0.09	1.12 ± 0.11	2.24 ± 0.22	2.81 ± 0.28	2.41 ± 0.24	4.78 ± 0.48	3.91 ± 0.39	8.43 ± 0.84	7.51 ± 0.75	6.93 ± 0.70	9.05 ± 0.91
	Br	1.64 ± 0.08	0.08 ± 0.01	0.03 ± 0.003	0.35 ± 0.04	0.78 ± 0.08	0.78 ± 0.08	1.12 ± 0.12	1.49 ± 0.15	1.21 ± 0.12	2.11 ± 0.21	1.28 ± 0.13	1.69 ± 0.17	1.41 ± 0.14
	Ba	0.31 ± 0.03	0.10 ± 0.01	BDL *	0.2 ± 0.02	0.15 ± 0.02	BDL *	0.41 ± 0.04	0.12 ± 0.01	0.32 ± 0.03	0.64 ± 0.06	0.77 ± 0.08	0.59 ± 0.06	0.59 ± 0.06
	Mg	0.57 ± 0.06	0.05 ± 0.01	0.05 ± 0.01	0.28 ± 0.03	0.43 ± 0.04	0.95 ± 0.09	1.51 ± 0.15	0.64 ± 0.06	0.44 ± 0.04	2.01 ± 0.20	2.50 ± 0.25	2.10 ± 0.21	1.48 ± 0.15
	Si	12.00 ± 1.20	1.21 ± 0.12	0.40 ± 0.04	7.45 ± 0.75	6.15 ± 0.62	5.68 ± 0.57	3.19 ± 0.32	6.78 ± 0.68	7.28 ± 0.73	14.48 ± 1.45	13.92 ± 1.39	11.21 ± 1.12	12.1 ± 1.21
	Mn	0.01 ± 0.001	0.03 ± 0.003	0.03 ± 0.003	0.03 ± 0.003	0.03 ± 0.003	BDL *	BDL *	BDL *	BDL *	BDL *	BDL *	BDL *	BDL *
Sum		21.26	2.69	2.01	9.59	9.83	10.22	8.82	13.99	13.28	27.88	26.00	22.79	24.93

* BDL—below detection limit.

In order to investigate the morphology of the concentrate and intermediate grains obtained from the most effective option for preparing the feed for an electrostatic separator (option 2), and to determine the chemical composition in grain micro-areas, as well as to demonstrate the number and type of metal–plastic–ceramic or metal–metal compounds, photographs were taken using quadrant backscatter diffraction (QBSD) (Figures 5 and 6), and measurements were performed using EDS (Tables 4 and 5). The differences in grain contrast in these figures indicate their heterogeneous chemical composition. The lighter areas indicate the presence of elements with a higher atomic number, while the dark ones indicate the elements with a lower atomic number. However, one should take into account the possibility of accumulation of surface charges by plastics, which, in the case of electrification, can also appear as bright areas. The concentrate (Figure 5) contained mostly homogeneous grains, without contrast. There were also a few grains forming metal–metal or metal–plastic–ceramic compounds. On the other hand, in the intermediate (Figure 6), the opposite was true; mainly nonhomogeneous grains appeared—all grains are in two shades.

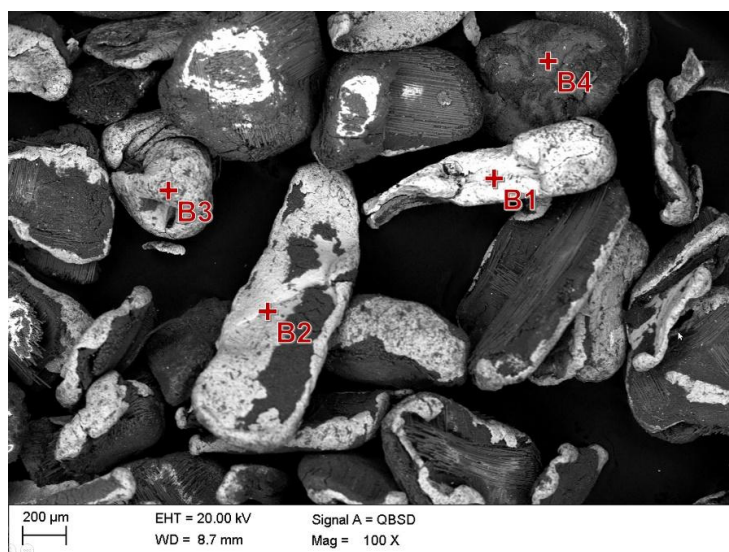


(a)

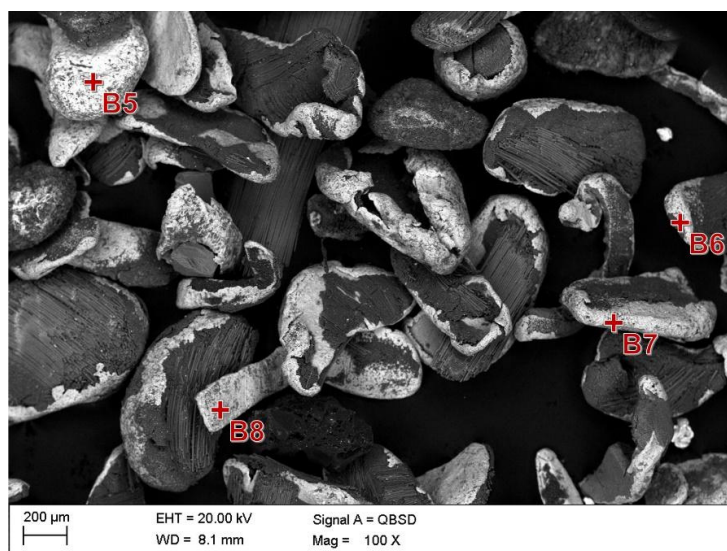


(b)

Figure 5. Concentrate from the electrostatic separation (SEM, QBSD mode (Table 4)) with marked EDS analysis points: (a) A1–A3 and (b) A5–A9.



(a)



(b)

Figure 6. Intermediate from the electrostatic separation (SEM, QBSD mode (Table 5)) with marked EDS analysis points: (a) B1–B4 and (b) B5–B8.

Table 4. Elemental concentrations (% at.) measured with EDS in the micro-areas marked in Figure 5.

Element	Point of Analysis								
	A1	A2	A3	A4	A5	A6	A7	A8	A9
Mg	-	-	-	6.2	-	-	-	-	-
Al	1.4	2.3	19.0	93.8	22.4	4.1	5.5	34.9	4.0
Si	-	1.0	46.8	-	-	-	-	3.6	1.7
Sc	-	-	-	-	-	-	0.2	-	0.2
Fe	-	-	-	-	3.2	-	-	-	-
Ni	-	-	-	-	26.4	-	-	-	37.0
Cu	98.6	96.8	5.0	-	12	-	3.1	50.9	45.8
Sn	-	-	-	-	-	95.9	89.7	10.7	10.6
Sb	-	-	-	-	-	-	1.6	-	0.7
Au	-	-	-	-	36	-	-	-	-
Na	-	-	1.0	-	-	-	-	-	-

Table 5. Elemental concentrations [% at.] measured with EDS in the micro-areas marked in Figure 6.

Element	Point of Analysis							
	B1	B2	B3	B4	B5	B6	B7	B8
Mg	-	-	1.5	-	-	-	1.8	-
Al	3.4	4.6	13.7	74.8	6.8	2.4	8.5	9.9
Si	-	-	20.4	4.6	-	1.2	-	1.2
Sc	-	-	-	-	0.3	-	-	-
Fe	-	-	23.1	1.7	-	-	-	-
Ni	4.3	-	2.0	-	-	-	-	-
Cu	17.2	95.4	26.9	10.6	5.9	96.4	89.7	87.3
Ag	1.2	-	-	-	2.5	-	-	-
Sn	73.9	-	-	6.6	83.6	-	-	-
Sb	-	-	-	-	0.8	-	-	-
Ca	-	-	4.7	1.3	-	-	-	-
Mn	-	-	0.2	-	-	-	-	-
S	-	-	0.5	-	-	-	-	-
Cl	-	-	-	0.3	-	-	-	1.6
Cr	-	-	6.7	-	-	-	-	-
Ba	-	-	0.2	-	-	-	-	-

The concentrations of the elements measured for the selected micro-areas of the concentrate grains (Figure 5) and the intermediate grains (Figure 6) are presented in Tables 4 and 5, respectively. The grains in the concentrate (Figure 5) below 300 μm in size were mainly homogeneous—they did not display any contrast. The patch grains and the irregular grains obtained were mainly made up of copper (e.g., points A1 and A2 in Figure 5). In the case of patch grains >600 μm in size (e.g., point A3 in Figure 5 marked on a grain with a diameter of 900 μm), an insufficient degree of metal release from nonvaluable elements is observed, from Si and Al in this case. The investigated micro-area of this grain consisted of 66% of these elements. In the remaining micro-areas of Si concentrate grains examined by means of EDS, it was absent or there was only a small amount (less than 5%). At point A5 (Figure 5, Table 4), the presence of gold was indicated for the elongated grain. It can be assumed that the grain came from gold-plated contacts. Elongated grains exhibit the highest purity, regardless of their size. It can therefore be assumed that these grains came mainly from contacts that had no connections with the PCB composite. Each tested area in the concentrate contained different amounts of aluminium.

On the basis of the presented analysis and observation of all concentrate grains, it can be summarised and generalised that metals contained in grains with size >800 μm are insufficiently released from plastic and ceramic materials. They should be ground again under the conditions in line with option 2.

Compared with the concentrate, the grains present in the intermediate were larger and ranged from about 500 μm to 1000 μm (Figure 6). The fibrous structure characteristic of ceramics can be seen in almost every grain. The grains' shape, their two-sided connections with plastic and ceramic materials, and their high copper content (Table 5) may indicate that these grains mainly come from the internal PCB layers. Due to the size of the grains, the intermediate can be reground or subjected to digestion with leaching solutions.

X-ray qualitative phase analysis was carried out for the concentrate and the intermediate also obtained from the most effective option for preparing the feed for an electrostatic separator (i.e., option 2). The analysis of the phase composition of the concentrate (Figure 7) did not indicate phases that could suggest the presence of impurities, nonvaluable elements, unlike that of the intermediate (Figure 8), where the diffraction lines from silicon were identified. Phases such as copper, tin, and CuSn (bronze) were identified in the concentrate (Figure 7), while in the intermediate, apart from silicon, copper and aluminium were also present. Due to the limited sensitivity of the method, the presence of other metallic/nonmetallic phases in small amounts cannot be excluded.

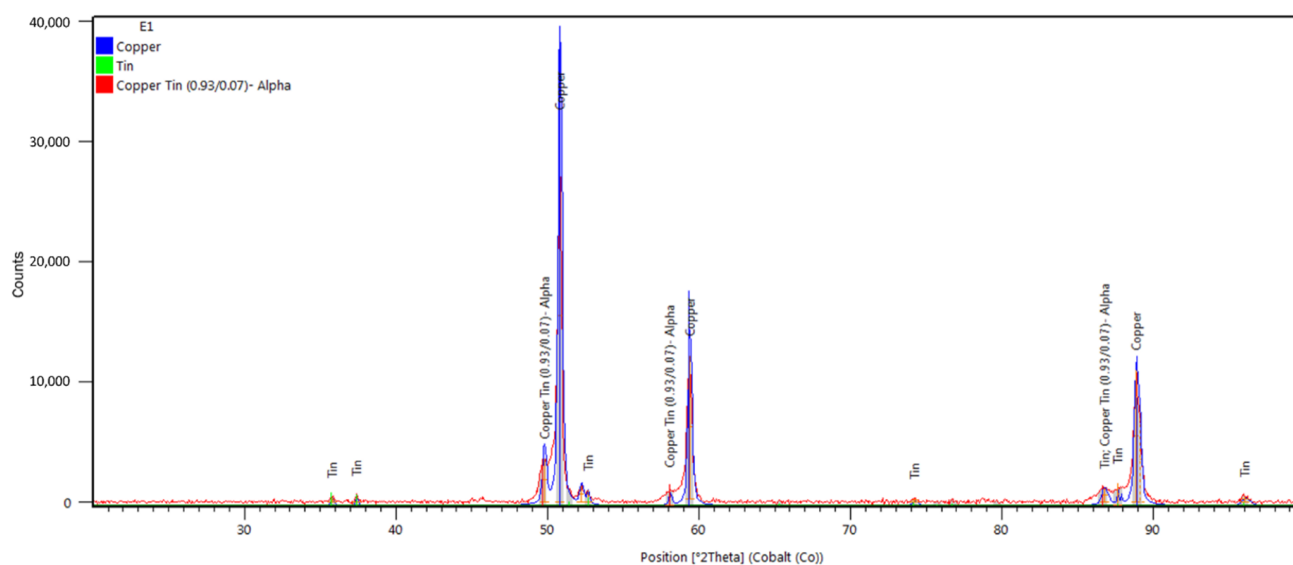


Figure 7. X-ray diffraction patterns of the concentrate.

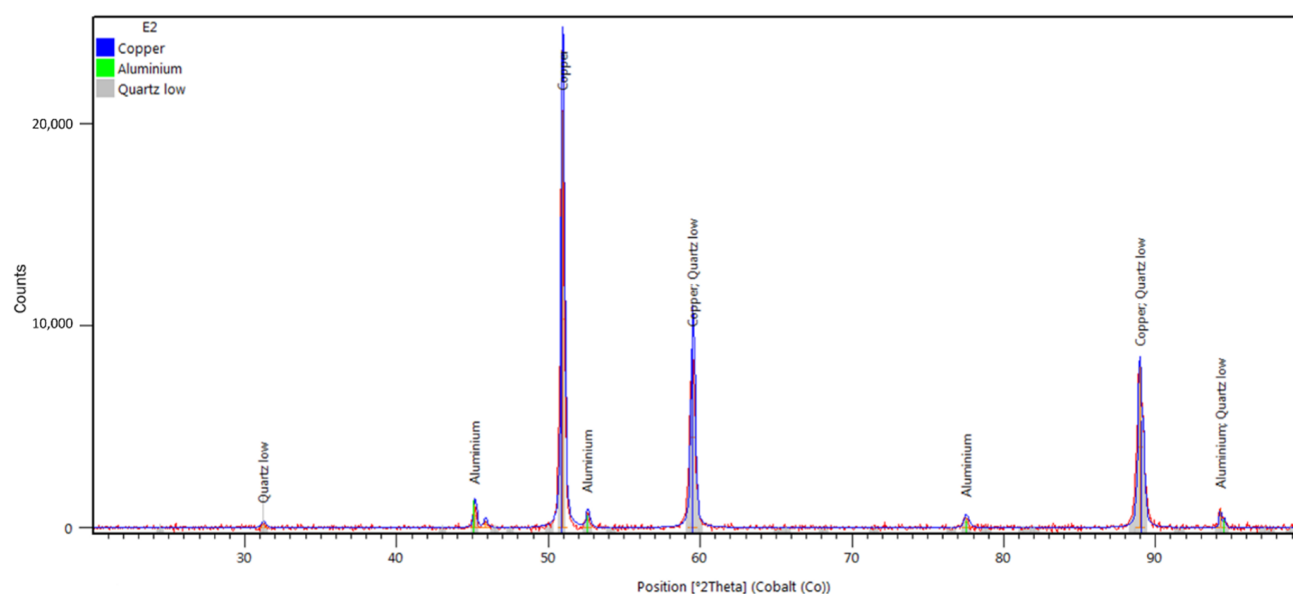


Figure 8. X-ray diffraction patterns of the intermediate.

4. Discussion

The obtained results of metal recovery efficiency tests using electrostatic separation for various options of PCB grinding confirm that the method and degree of grinding significantly affect the purity of the concentrate and waste, and thus the efficiency of the process. Significant indicators of the grinding degree were the limit dimensions of the ground grains, as well as the resulting level of metal release from plastic and ceramic materials.

According to the work of Li et al. [7], full metal release occurs for grains <0.6 mm, while Kaya [24] reports that it occurs only for grains <0.15 mm. In both of the above-mentioned papers, the research involved multistage grinding in hammer mills and the use of various PCBs, which could have had an impact on the results. Based on the results of the research presented in this article, it can be seen that the complete release of metals from plastic and ceramic materials occurred for grains <0.3 mm and, to a lesser extent, for grains smaller than 0.8 mm. Grinding was carried out with a knife mill, and the feed was

cooled to cryogenic temperature. So far, little research was done to assess the efficiency of PCB grinding using knife mills and cryogenic temperatures in detail. Grinding, cooling the feed to cryogenic temperature, and the preprocessing steps are energy-consuming processes. The validity of using these methods should be confirmed by economic analysis and compared with other methods for recovering useful substances from PCBs.

It can be assumed that the degree of grinding for which the metals are fully released depends, to some extent, on the type of PCB. At this point, it should be added after authors Li et al. [7] and Wu et al. [40] that electrostatic separation may be effective for grains <1.2 mm. In addition, the separation efficiency is influenced by the optimisation of the process (i.e., for the drum electrostatic separator, the adjustment of the voltage, the shaft rotational speed, and the load of the separator). These parameters were not analysed in this paper.

In this work, the separation efficiency was analysed in terms of product yield, the penetration of inappropriate grains into individual products, and the presence of mixed grains in them (i.e., conglomerates—solid metal–plastic–ceramic compounds). The concentrate from electrostatic separation for the option of grinding using a 3 mm screen perforation in the knife mill was the one most contaminated with plastic and ceramic materials. In this case, a fairly large amount of metals also penetrated into the waste. This is explained by the fact that as much as 38.5% of the grains after grinding were larger than 1 mm. In the grinding option using a 2 mm screen perforation, the content of grains >1 mm was 11.5%. This resulted in an increase in the content of metals in the concentrate, but not a sufficient one. The low separation efficiency for these grinding options could also be caused by an insufficient electrostatic force. According to Wu et al. [40], a 20 kV voltage is suitable for efficient electrostatic separation of fine grains. For larger ones, it may be insufficient, and increasing the voltage may negatively affect the overall efficiency of the process.

A much better efficiency of recovering metals from PCBs was obtained for the options of grinding using a screen with a 1 mm perforation, without and with cooling the feed to cryogenic temperatures, respectively. In these cases, grains >1 mm were not present in the grinding products. The share of grains <0.5 mm was substantial. The yields of separation products for these options were very similar, but for the option with a reduced feed temperature per grain mill, they were generally slightly smaller. For this case, the purity of the concentrate and waste was the highest. Only small amounts of fine metal grains (below 200 µm) that were trapped in the fibrous structure of the glass fibre grains were identified in the waste. It can therefore be concluded that cooling the material to cryogenic temperatures has a positive effect on the size and shape of the grains, and thus, in line with the conclusions of Lu et al. [44], on the recovery of metals from PCBs. It should be added that the cooled material was ground much faster, and the degree of metal release was higher.

It could be assumed that due to the multilayer structure of PCBs, it is advantageous to obtain the smallest possible grain [31,46]. Wu et al., however, report [40] that very fine grains below 0.091–0.125 mm may contribute to ineffective electrostatic separation caused by the grain aggregation effect on the drum and electrode surface. According to Wu et al. [56], this effect may have a significant impact on the stability of the separation process. Considering the above, in order to obtain the appropriate electrostatic separation efficiency, a very narrow grain class should be used with the separator. The settling of dust made of plastic and ceramic materials on the electrode surface was observed in the research papers presented in this paper. On the other hand, aggregation on the drum surface was very limited when using cryogenic temperatures for the preparation of the feed.

For the concentrate obtained from electrostatic separation, for the option of PCB grinding using cryogenic temperatures and 1 mm screen perforation, the value of valuable metals that can be obtained was estimated on the basis of the London Metal Exchange. The metal content in the concentrate for this grinding option is shown (based on Table 3) in Figure 9. The estimated value refers to pure metals and does not include the costs required for PCB processing. As can be seen from Table 6, gold and copper have the decisive share

in the final value, accounting for 39% and 37% of the total, respectively, followed by tin at 15.5% and silver at 6%. Due to the low gold content of PCBs, the recovery process should be adapted to minimise the loss of this metal. In this case, the PCB grinding process may be a critical stage. In order to improve the efficiency of copper recovery, which creates numerous connections with plastic and ceramic materials due to the PCB structure, the grinding process should be carried out in such a way as to obtain the highest possible release of this metal.

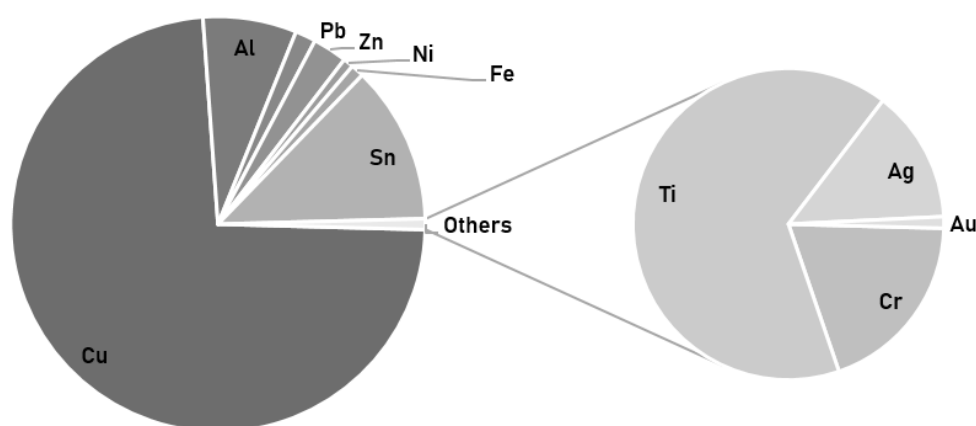


Figure 9. Metal content in the concentrate obtained from electrostatic separation for the option of PCB grinding using cryogenic temperatures and 1 mm screen perforation.

Table 6. The value of metals recoverable from the concentrate obtained from electrostatic separation for the option of PCB grinding using cryogenic temperatures and 1 mm screen perforation.

Metal	Price *, (\$/Mg)	Metal Content in the Concentrate (Data from Table 3), %	Metal Recovery Level Related to the Initial PCB Mass (after Dismantling), %	Prices of Metals Obtained from 100 g of PCB, \$
Cu	7635	68.5	17.95	1.4
Al	1986	6.82	1.79	0.035
Pb	2063	1.5	0.39	0.008
Zn	2762	2.5	0.66	0.018
Ni	16,390	0.75	0.20	0.032
Fe	553	0.95	0.25	0.001
Sn	19,128	11.5	3.01	0.576
Ag	7.91×10^5	0.1074	0.0281	0.223
Au	6.01×10^7	0.0092	0.0024	1.4
			Suma, \$	3.7

* According to the London Metal Exchange (December 2020).

At high temperatures occurring in the mill's working chamber, when cryogenic temperatures are not used to prepare the feed, gold becomes plastic, which may lead to coating of the mill elements and other grains of harder metals. When liquid nitrogen was used to cool the feed, this unfavourable effect was minimised.

5. Conclusions

The use of a knife mill with the use of a 1 mm screen perforation along with cooling the feed to cryogenic temperature significantly improves the full release of useful components from PCBs. After grinding, the mixture of fine grains can be transferred to the electrostatic separation process in order to separate metals in the free state from plastics and ceramic materials, while before grinding, hazardous products, such as batteries, capacitors, and radiators, must be disassembled from the PCBs. Similar directions of activities in the field of PCB recycling were presented by Vermesan et al. [1]. This is in line with the circular

economy policy. In this way, metals can be recovered (economic benefits), but also the negative impact of human activity on the environment can be reduced by limiting the extraction and processing of metal ores and the amount of waste.

The recovered mixture of metals, the concentrate from the electrostatic separation process, can be transferred to metallurgical processing, where metals are produced along with the concentrate from the processing of nonferrous metal ores, while plastic and ceramic materials, the waste from the electrostatic separation, can be used as secondary raw materials for the production of various components/prefabricates. The purity of the concentrate and the waste obtained from electrostatic separation was satisfactory, and the proportion of the intermediate, in which the conglomerates of solid metal–plastic–ceramic compounds were present, was very low. The yield of the concentrate and the waste amounted to 26.2% and 71.0%, respectively, and their purity, reflected in the content of the identified valuable metals, was at the level of 93.3% and 0.5%, respectively.

Author Contributions: Research concept, T.S. and D.M.F.; conduct of the process of grinding and electrostatic separation, D.M.F.; XRD analysis, P.M.N.; analysis of grinding, T.S. and B.T.; analysis of the yield of separation products and their density, D.M.F., P.M., and D.K.; microscopic and ICP analysis, D.M.F. and T.S.; investigation, T.S. and D.M.F.; writing—original draft preparation, D.M.F. and T.S.; writing—review and editing, D.M.F., T.S., P.M.N., B.T., D.K., and P.M. All authors have read and agreed to the published version of the manuscript.

Funding: The project was funded under the statutory financial grant BK-06/050/BK_20/0101 for the year 2020 of the Faculty of Mining, Safety Engineering and Industrial Automation, Silesian University of Technology.

Institutional Review Board Statement: Not applicable.

Informed Consent Statement: Not applicable.

Data Availability Statement: Data sharing not applicable.

Acknowledgments: The authors thank Krzysztof Matus for SEM characterization.

Conflicts of Interest: The authors declare no conflict of interest. The funders had no role in the design of the study; in the collection, analyses, or interpretation of data; in the writing of the manuscript; or in the decision to publish the results.

References

1. Vermeşan, H.; Tiuc, A.-E.; Purcar, M. Advanced Recovery Techniques for Waste Materials from IT and Telecommunication Equipment Printed Circuit Boards. *Sustainability* **2019**, *12*, 74. [\[CrossRef\]](#)
2. Kumar, V.; Lee, J.; Jeong, J.; Jha, M.K.; Kim, B.; Singh, R. Recycling of Printed Circuit Boards (PCBs) to Generate Enriched Rare Metal Concentrate. *J. Ind. Eng. Chem.* **2015**, *21*, 805–813. [\[CrossRef\]](#)
3. Sohaili, J.; Muniyandi, S.K.; Mohamad, S.S. A Review on Printed Circuit Board Recycling Technology. *J. Emerg. Trends Eng. Appl. Sci.* **2012**, *3*, 12–18.
4. Tsydenova, O.; Bengtsson, M. Chemical Hazards Associated with Treatment of Waste Electrical and Electronic Equipment. *Waste Manag.* **2011**, *31*, 45–58. [\[CrossRef\]](#)
5. Johnson, J.; Harper, E.M.; Lifset, R.; Graedel, T.E. Supporting Information for “Dining at the Periodic Table: Metals” Concentrations as They Relate to Recycling. *Environ. Sci. Technol.* **2007**, *41*, 1759–1765. [\[CrossRef\]](#) [\[PubMed\]](#)
6. Tuncuk, A.; Stazi, V.; Akcil, A.; Yazici, E.Y.; Deveci, H. Aqueous Metal Recovery Techniques from E-Scrap: Hydrometallurgy in Recycling. *Miner. Eng.* **2012**, *25*, 28–37. [\[CrossRef\]](#)
7. Li, J.; Lu, H.; Guo, J.; Xu, Z.; Zhou, Y. Recycle Technology for Recovering Resources and Products from Waste Printed Circuit Boards. *Environ. Sci. Technol.* **2007**, *41*, 1995–2000. [\[CrossRef\]](#)
8. Dascalescu, L.; Iuga, A.; Morar, R. Corona–Electrostatic Separation: An Efficient Technique for the Recovery of Metals and Plastics From Industrial Wastes. *Magn. Electr. Sep.* **1900**, *4*, 059037. [\[CrossRef\]](#)
9. Huang, K.; Guo, J.; Xu, Z. Recycling of Waste Printed Circuit Boards: A Review of Current Technologies and Treatment Status in China. *J. Hazard. Mater.* **2009**, *164*, 399–408. [\[CrossRef\]](#) [\[PubMed\]](#)
10. Kumar, A.; Holuszko, M.E.; Janke, T. Characterization of the Non-Metal Fraction of the Processed Waste Printed Circuit Boards. *Waste Manag.* **2018**, *75*, 94–102. [\[CrossRef\]](#) [\[PubMed\]](#)
11. Weil, E.D.; Levchik, S. A Review of Current Flame Retardant Systems for Epoxy Resins. *J. Fire Sci.* **2004**, *22*, 25–40. [\[CrossRef\]](#)
12. Muniyandi, S.K.; Sohaili, J.; Hassan, A. Encapsulation of Nonmetallic Fractions Recovered from Printed Circuit Boards Waste with Thermoplastic. *J. Air Waste Manag. Assoc.* **2014**, *64*, 1085–1092. [\[CrossRef\]](#)

13. Duan, H.; Hu, J.; Yuan, W.; Wang, Y.; Yu, D.; Song, Q.; Li, J. Characterizing the Environmental Implications of the Recycling of Non-Metallic Fractions from Waste Printed Circuit Boards. *J. Clean. Prod.* **2016**, *137*, 546–554. [\[CrossRef\]](#)
14. Bizzo, W.; Figueiredo, R.; de Andrade, V. Characterization of Printed Circuit Boards for Metal and Energy Recovery after Milling and Mechanical Separation. *Materials* **2014**, *7*, 4555–4566. [\[CrossRef\]](#)
15. Charles, R.G.; Douglas, P.; Hallin, I.L.; Matthews, I.; Liversage, G. An Investigation of Trends in Precious Metal and Copper Content of RAM Modules in WEEE: Implications for Long Term Recycling Potential. *Waste Manag.* **2017**, *60*, 505–520. [\[CrossRef\]](#) [\[PubMed\]](#)
16. Cayumil, R.; Khanna, R.; Rajarao, R.; Mukherjee, P.S.; Sahajwalla, V. Concentration of Precious Metals during Their Recovery from Electronic Waste. *Waste Manag.* **2016**, *57*, 121–130. [\[CrossRef\]](#) [\[PubMed\]](#)
17. Schluep, M.; Hagelueken, C.; Kuehr, R.; Magalini, F.; Maurer, C. Recycling—from e-Waste to Resources. In *Sustainable Innovation and Technology Transfer Industrial Sector Studies*; UNEP and STeP: Nairobi, Kenya; Bonn, Germany, 2006.
18. Mao, S.; Kang, Y.; Zhang, Y.; Xiao, X.; Zhu, H. Fractional Grey Model Based on Non-Singular Exponential Kernel and Its Application in the Prediction of Electronic Waste Precious Metal Content. *ISA Trans.* **2020**, *107*, 12–26. [\[CrossRef\]](#) [\[PubMed\]](#)
19. Hagelüken, C. Recycling of Electronic Scrap at Umicore's Integrated Metals Smelter and Refinery. *World Metall. Erzmetall* **2006**, *59*, 152–161.
20. Song, Q.; Zeng, X.; Li, J.; Duan, H.; Yuan, W. Environmental Risk Assessment of CRT and PCB Workshops in a Mobile E-Waste Recycling Plant. *Environ. Sci. Pollut. Res.* **2015**, *22*, 12366–12373. [\[CrossRef\]](#)
21. Dervišević, I.; Minić, D.; Kamberović, Ž.; Čosović, V.; Ristić, M. Characterization of PCBs from Computers and Mobile Phones, and the Proposal of Newly Developed Materials for Substitution of Gold, Lead and Arsenic. *Environ. Sci. Pollut. Res.* **2013**, *20*, 4278–4292. [\[CrossRef\]](#) [\[PubMed\]](#)
22. Niu, Q.; Xiang, D.; Liu, X.; Duan, G.; Shi, C. The Recycle Model of Printed Circuit Board and Its Economy Evaluation. In *Proceedings of the 2007 IEEE International Symposium on Electronics and the Environment*, Orlando, FL, USA, 7–10 May 2007; IEEE: Orlando, FL, USA, 2007; pp. 106–111.
23. Guo, C.; Wang, H.; Liang, W.; Fu, J.; Yi, X. Liberation Characteristic and Physical Separation of Printed Circuit Board (PCB). *Waste Manag.* **2011**, *31*, 2161–2166. [\[CrossRef\]](#)
24. Kaya, M. Recovery of Metals and Nonmetals from Electronic Waste by Physical and Chemical Recycling Processes. *Waste Manag.* **2016**, *57*, 64–90. [\[CrossRef\]](#)
25. Leung, A.O.W.; Luksemburg, W.J.; Wong, A.S.; Wong, M.H. Spatial Distribution of Polybrominated Diphenyl Ethers and Polychlorinated Dibenzo-p-Dioxins and Dibenzofurans in Soil and Combusted Residue at Guiyu, an Electronic Waste Recycling Site in Southeast China. *Environ. Sci. Technol.* **2007**, *41*, 2730–2737. [\[CrossRef\]](#)
26. Qiu, R.; Lin, M.; Ruan, J.; Fu, Y.; Hu, J.; Deng, M.; Tang, Y.; Qiu, R. Recovering Full Metallic Resources from Waste Printed Circuit Boards: A Refined Review. *J. Clean. Prod.* **2020**, *244*, 118690. [\[CrossRef\]](#)
27. Xiang, D.; Mou, P.; Wang, J.; Duan, G.; Zhang, H.C. Printed Circuit Board Recycling Process and Its Environmental Impact Assessment. *Int. J. Adv. Manuf. Technol.* **2007**, *34*, 1030–1036. [\[CrossRef\]](#)
28. Argumede-Delira, R.; Gómez-Martínez, M.J.; Soto, B.J. Gold Bioleaching from Printed Circuit Boards of Mobile Phones by *Aspergillus Niger* in a Culture without Agitation and with Glucose as a Carbon Source. *Metals* **2019**, *9*, 521. [\[CrossRef\]](#)
29. Drzymała, J.; Swatek, A. *Mineral Processing: Foundations of Theory and Practice of Mineralurgy*; University of Technology: Wrocław, Poland, 2007; ISBN 978-83-7493-362-9.
30. Tatariants, M.; Yousef, S.; Sidoraviciute, R.; Denafas, G.; Bendikiene, R. Characterization of Waste Printed Circuit Boards Recycled Using a Dissolution Approach and Ultrasonic Treatment at Low Temperatures. *RSC Adv.* **2017**, *7*, 37729–37738. [\[CrossRef\]](#)
31. Forti, V.; Baldé, C.P.; Kuehr, R.; Bel, G. *The Global E-Waste Monitor 2020: Quantities, Flows and the Circular Economy Potential*; United Nations University (UNU)/United Nations Institute for Training and Research (UNITAR)—Co-Hosted SCYCLE Programme, International Telecommunication Union (ITU) & International Solid Waste Association (ISWA): Bonn, Germany; Geneva, Switzerland; Rotterdam, The Netherlands, 2020; p. 120.
32. Bidini, G.; Fantozzi, F.; Bartocci, P.; D'Alessandro, B.; D'Amico, M.; Laranci, P.; Scozza, E.; Zagaroli, M. Recovery of Precious Metals from Scrap Printed Circuit Boards through Pyrolysis. *J. Anal. Appl. Pyrolysis* **2015**, *111*, 140–147. [\[CrossRef\]](#)
33. LaDou, J. Printed Circuit Board Industry. *Int. J. Hyg. Environ. Health* **2006**, *209*, 211–219. [\[CrossRef\]](#)
34. Ernst, T.; Popp, R.; Wolf, M.; van Eldik, R. Analysis of Eco-Relevant Elements and Noble Metals in Printed Wiring Boards Using AAS, ICP–AES and EDXRF. *Anal. Bioanal. Chem.* **2003**, *375*, 805–814. [\[CrossRef\]](#)
35. Koyanaka, S.; Endoh, S.; Ohya, H. Effect of Impact Velocity Control on Selective Grinding of Waste Printed Circuit Boards. *Adv. Powder Technol.* **2006**, *17*, 113–126. [\[CrossRef\]](#)
36. Li, J.; Xu, Z.; Zhou, Y. Application of Corona Discharge and Electrostatic Force to Separate Metals and Nonmetals from Crushed Particles of Waste Printed Circuit Boards. *J. Electrostat.* **2007**, *65*, 233–238. [\[CrossRef\]](#)
37. Khaliq, A.; Rhamdhani, M.; Brooks, G.; Masood, S. Metal Extraction Processes for Electronic Waste and Existing Industrial Routes: A Review and Australian Perspective. *Resources* **2014**, *3*, 152–179. [\[CrossRef\]](#)
38. Dascalescu, L.; Tilmatine, A.; Aman, F.; Mihailescu, M. Optimization of Electrostatic Separation Processes Using Response Surface Modeling. *IEEE Trans. Ind. Appl.* **2004**, *40*, 53–59. [\[CrossRef\]](#)
39. Zenkiewicz, M.; Zuk, T. Physical basis of tribocharging and electrostatic separation of plastics. *Polimery* **2014**, *59*, 314–323. [\[CrossRef\]](#)

40. Wu, J.; Li, J.; Xu, Z. Electrostatic Separation for Recovering Metals and Nonmetals from Waste Printed Circuit Board: Problems and Improvements. *Environ. Sci. Technol.* **2008**, *42*, 5272–5276. [[CrossRef](#)]
41. Wei, J.; Realff, M.J. Design and Optimization of Free-Fall Electrostatic Separators for Plastics Recycling. *AIChE J.* **2003**, *49*, 3138–3149. [[CrossRef](#)]
42. Tilmatine, A.; Medles, K.; Bendimerad, S.-E.; Boukholda, F.; Dascalescu, L. Electrostatic Separators of Particles: Application to Plastic/Metal, Metal/Metal and Plastic/Plastic Mixtures. *Waste Manag.* **2009**, *29*, 228–232. [[CrossRef](#)] [[PubMed](#)]
43. Hou, S.; Wu, J.; Qin, Y.; Xu, Z. Electrostatic Separation for Recycling Waste Printed Circuit Board: A Study on External Factor and a Robust Design for Optimization. *Environ. Sci. Technol.* **2010**, *44*, 5177–5181. [[CrossRef](#)] [[PubMed](#)]
44. Lu, H.; Li, J.; Guo, J.; Xu, Z. Movement Behavior in Electrostatic Separation: Recycling of Metal Materials from Waste Printed Circuit Board. *J. Mater. Process. Technol.* **2008**, *197*, 101–108. [[CrossRef](#)]
45. Li, J.; Zhou, Q.; Xu, Z. Real-Time Monitoring System for Improving Corona Electrostatic Separation in the Process of Recovering Waste Printed Circuit Boards. *Waste Manag. Res.* **2014**, *32*, 1227–1234. [[CrossRef](#)] [[PubMed](#)]
46. Sanapala, R. Characterization of FR-4 Printed Circuit Board Laminates Before and After Exposure to Lead-Free Soldering Conditions. Ph.D. Thesis, University of Maryland, College Park, MD, USA, 2008.
47. Franke, D.; Suponik, T. Metals Recovery from E-Scrap Using Gravity, Electrostatic and Magnetic Separations. *IOP Conf. Ser. Mater. Sci. Eng.* **2019**, *545*, 012016. [[CrossRef](#)]
48. Lee, J.; Kim, Y.; Lee, J. Disassembly and Physical Separation of Electric/Electronic Components Layered in Printed Circuit Boards (PCB). *J. Hazard. Mater.* **2012**, *241–242*, 387–394. [[CrossRef](#)] [[PubMed](#)]
49. Available online: www.testchem.pl/en/testchem-products/sample-preparing/grinders-and-crushers/knife-lab-grinders/ (accessed on 4 December 2020).
50. Franke, D.; Suponik, T.; Nuckowski, P.M.; Gołombek, K.; Hyra, K. Recovery of Metals from Printed Circuit Boards By Means of Electrostatic Separation. *Manag. Syst. Prod. Eng.* **2020**, *28*, 213–219. [[CrossRef](#)]
51. Suponik, T.; Franke, D.; Nuckowski, P. Electrostatic and Magnetic Separations for the Recovery of Metals from Electronic Waste. *IOP Conf. Ser. Mater. Sci. Eng.* **2019**, *641*, 012017. [[CrossRef](#)]
52. Wu, W.; Liu, X.; Zhang, X.; Zhu, M.; Tan, W. Bioleaching of Copper from Waste Printed Circuit Boards by Bacteria-Free Cultural Supernatant of Iron-Sulfur-Oxidizing Bacteria. *Bioresour. Bioprocess.* **2018**, *5*, 10. [[CrossRef](#)]
53. Pham, H.Q.; Marks, M.J. Epoxy Resins. In *Ullmann's Encyclopedia of Industrial Chemistry*; Wiley-VCH Verlag GmbH & Co. KGaA, Ed.; Wiley-VCH Verlag GmbH & Co. KGaA: Weinheim, Germany, 2005; pp. 155–244. ISBN 978-3-527-30673-2.
54. Sood, B.; Sanapala, R.; Das, D.; Pecht, M.; Huang, C.Y.; Tsai, M.Y. Comparison of Printed Circuit Board Property Variations in Response to Simulated Lead-Free Soldering. *IEEE Trans. Electron. Packag. Manuf.* **2010**, *33*, 98–111. [[CrossRef](#)]
55. Sood, B.; Pecht, M. The Effect of Epoxy/Glass Interfaces on CAF Failures in Printed Circuit Boards. *Microelectron. Reliab.* **2018**, *82*, 235–243. [[CrossRef](#)]
56. Wu, J.; Qin, Y.; Zhou, Q.; Xu, Z. Impact of Nonconductive Powder on Electrostatic Separation for Recycling Crushed Waste Printed Circuit Board. *J. Hazard. Mater.* **2009**, *164*, 1352–1358. [[CrossRef](#)] [[PubMed](#)]